(2)

David W. Taylor Naval Ship Research and Development Center
Bethesda, MD 20084–5000

DTNSRDC/ASED-86/04 December 1986

Aviation and Surface Effects Department
Research and Development Report

Low Reynolds Number Experiments on the Wortmann FX61-184 Airfoil

by
John J. Deily
William D. McGrory

MAJOR DTRC TECHNICAL COMPONENTS

CODE 011 DIRECTOR OF TECHNOLOGY, PLANS AND ASSESSMENT

12 SHIP SYSTEMS INTEGRATION DEPARTMENT

14 SHIP ELECTROMAGNETIC SIGNATURES DEPARTMENT

15 SHIP HYDROMECHANICS DEPARTMENT

16 AVIATION DEPARTMENT

17 SHIP STRUCTURES AND PROTECTION DEPARTMENT

18 COMPUTATION, MATHEMATICS & LOGISTICS DEPARTMENT

19 SHIP ACOUSTICS DEPARTMENT

27 PROPULSION AND AUXILIARY SYSTEMS DEPARTMENT

28 SHIP MATERIALS ENGINEERING DEPARTMENT

DTRC ISSUES THREE TYPES OF REPORTS:

1. **DTRC reports, a formal series,** contain information of permanent technical value. They carry a consecutive numerical identification regardless of their classification or the originating department.

2. **Departmental reports, a semiformal series,** contain information of a preliminary, temporary, or proprietary nature or of limited interest or significance. They carry a departmental alphanumerical identification.

3. **Technical memoranda, an informal series,** contain technical documentation of limited use and interest. They are primarily working papers intended for internal use. They carry an identifying number which indicates their type and the numerical code of the originating department. Any distribution outside DTRC must be approved by the head of the originating department on a case-by-case basis.

UNCLASSIFIED

SECURITY CLASSIFICATION OF THIS PAGE

REPORT DOCUMENTATION PAGE

1a REPORT SECURITY CLASSIFICATION UNCLASSIFIED	1b RESTRICTIVE MARKINGS
2a SECURITY CLASSIFICATION AUTHORITY	3 DISTRIBUTION / AVAILABILITY OF REPORT Approved for public release; distribution is unlimited.
2b DECLASSIFICATION / DOWNGRADING SCHEDULE	
4 PERFORMING ORGANIZATION REPORT NUMBER(S) DTNSRDC/ASED-86/04	5 MONITORING ORGANIZATION REPORT NUMBER(S)
6a NAME OF PERFORMING ORGANIZATION David W. Taylor Naval Ship R&D Center 6b OFFICE SYMBOL (If applicable) Code 1603	7a NAME OF MONITORING ORGANIZATION Naval Air Development Center Code 605
6c ADDRESS (City, State, and ZIP Code) Bethesda, MD 20084-5000	7b ADDRESS (City, State, and ZIP Code) Warminster, PA 18974-5000
8a NAME OF FUNDING / SPONSORING ORGANIZATION 8b OFFICE SYMBOL (If applicable)	9 PROCUREMENT INSTRUMENT IDENTIFICATION NUMBER
8c ADDRESS (City, State, and ZIP Code)	10 SOURCE OF FUNDING NUMBERS PROGRAM ELEMENT NO. 62766N; PROJECT NO; TASK NO.; WORK UNIT ACCESSION NO. DN506138

11 TITLE (Include Security Classification)

Low Reynolds Number Experiments on the Wortmann FX61-184 Airfoil

12 PERSONAL AUTHOR(S)
Deily, John J. and McGrory, William D.

13a TYPE OF REPORT	13b TIME COVERED	14 DATE OF REPORT (Year, Month, Day)	15 PAGE COUNT
Final	FROM 8601 TO 8609	1986 December	38

16 SUPPLEMENTARY NOTATION

17 COSATI CODES			18 SUBJECT TERMS (Continue on reverse if necessary and identify by block number)
FIELD	GROUP	SUB-GROUP	Wortmann Airfoil; Chord Reynolds Number; Wind tunnel tests; Low Reynolds Number

19 ABSTRACT (Continue on reverse if necessary and identify by block number)

A series of low-speed, two-dimensional wind tunnel experiments were conducted on a Wortmann FX61-184 airfoil. The airfoil chord was one foot, and chord Reynolds number varied from approximately 0.25 million to 1.0 million at tunnel dynamic pressures of 2.5 to 30 pounds/square foot. Airfoil surface, wake, and tunnel dynamic pressure measurements were taken to determine airfoil performance characteristics. The major experimental parameters varied were Reynolds number and angle of attack. Experimental results are compared with theoretical predictions and previous wind tunnel data at a Reynolds number of 1×10^6.

20 DISTRIBUTION / AVAILABILITY OF ABSTRACT ☐ UNCLASSIFIED/UNLIMITED ☒ SAME AS RPT ☐ DTIC USERS	21 ABSTRACT SECURITY CLASSIFICATION UNCLASSIFIED
22a NAME OF RESPONSIBLE INDIVIDUAL John J. Deily	22b TELEPHONE (Include Area Code) (202) 227-1177 22c OFFICE SYMBOL Code 1603

DD FORM 1473, 84 MAR 83 APR edition may be used until exhausted. All other editions are obsolete

SECURITY CLASSIFICATION OF THIS PAGE
UNCLASSIFIED

CONTENTS

FIGURES

FIGURES (Continued)

TABLES

NOTATION

c	Airfoil chord length, ft
C_a	Section axial force coefficient, $(C_{p_{upper}} - C_{p_{lower}})d(y/c)$
C_d	Section drag coefficient, (Eq. 1)
C_ℓ	Section lift coefficient, (Eq. 2)
C_n	Section normal force coefficient, $(C_{p_{lower}} - C_{p_{upper}})d(y/c)$,
$C_{m_{c/4}}$	Section quarter-chord moment coefficient, (Eq. 3)
C_p	Pressure coefficient, $(p-p_\infty)/q_\infty$
M_∞	Free-stream Mach number
P_∞	Free-stream static pressure, lb/ft^2
P_2	Local wake rake static pressure, lb/ft^2
P_{o_2}	Local wake rake total pressure, lb/ft^2
P_{o_∞}	Free-stream total pressure, lb/ft^2
q_∞	Free-stream dynamic pressure, lb/ft^2
Re	Chord Reynolds number
V_∞	Free-stream velocity, ft/sec
x	Coordinate measured parallel to chord line, in.
y	Vertical distance measured from first wake rake tube, ft
z	Coordinate measured normal to chord line, in.
α	Angle of attack, deg
γ	Ratio of specicic heats (1.4 for air)

Subscripts

u	Upper
l	Lower

ABSTRACT

A series of low-speed, two-dimensional wind tunnel experiments were conducted on a Wortmann FX61-184 airfoil. The airfoil chord was one foot, and chord Reynolds number varied from approximately 0.25 million to 1.0 million at tunnel dynamic pressures of 2.5 to 30 pounds/square foot. Airfoil surface, wake, and tunnel dynamic pressure measurements were taken to determine airfoil performance characteristics. The major experimental parameters varied were Reynolds number and angle of attack. Experimental results are compared with theoretical predictions and previous wind tunnel data at a Reynolds number of 1×10^6.

ADMINISTRATIVE INFORMATION

This work was conducted by the New Vehicle Office (Code 1603) of the Aviation and Surface Effects Department at the David W. Taylor Naval Ship Research and Development Center (DTNSRDC). Funding for the model design, construction, and wind tunnel test was provided by the Naval Air Development Center, Aircraft and Crew Systems Technology Directorate, under Program Element 62766N, Work Unit 1-1603-305.

INTRODUCTION

An experimental investigation of a two-dimensional Wortmann FX61-184 airfoil was conducted in the 8- by 10-ft south subsonic wind tunnel at DTNSRDC. The airfoil is an 18-percent-thick, single element airfoil designed for low drag and large lift-to-drag ratios. The objective of this investigation was to determine the section characteristics for a range of Reynolds numbers from 0.5×10^6 to 1.0×10^6. Previously obtained wind tunnel data for a model based on this airfoil were at a minimum Reynolds number of 1.0×10^6 (Ref. 1).

The FX61-184 airfoil was tested over a chord Reynolds number range of approximately 0.25 to 1.0×10^6 and an angle-of-attack range of -6 to 15 deg. Lift, drag, and moment coefficients were calculated from airfoil and wake rake pressure measurements. Flow visualization was used to detect boundary-layer transition and separation.

MODEL DESCRIPTION

The airfoil section used in this experiment is a modified Wortmann FX61-184 airfoil; see Fig. 1. The airfoil was designed with a cusped trailing edge; therefore, construction of the model required that the "design" coordinates be altered to provide a trailing edge of finite thickness. The design airfoil section coordinates are listed in Table 1. To allow for a finite thickness trailing edge suitable for machining, additional thickness was added to the design thickness distribution. Beginning at midchord, a linearly increasing amount of thickness was added to both the upper and lower surfaces of the design airfoil. This resulted in model coordinates with a trailing edge thickness of 0.03 in. (0.25 percent of chord). Model section coordinates are listed in Table 2.

The model has a 12-in. chord and a 36-in. span, and was machined from a single piece of aluminum stock. Sixty-eight static pressure orifices are flush-mounted on the airfoil surface; see Fig. 2. Of these orifices, 66 are in a staggered arrangement about a chordwise line 6 in. to port of the midspan. A contoured access panel was cut in the lower surface to facilitate the installation of pressure taps. These chordwise taps are located off midspan so that any disturbances in the flow due to the pressure taps and access panel are not transmitted to the wake rake located 6 in. to starboard of midspan. Two static pressure orifices are located 6 in. to starboard of midspan at 50-percent chord. One tap is on the upper surface, and the second is on the lower surface. These taps were used to check the spanwise uniformity of the flow.

EXPERIMENTAL SETUP AND INSTRUMENTATION

The airfoil was installed at the vertical center of the 3- by 8-ft test section formed by two parallel inserts in the DTNSRDC south 8- by 10-ft wind tunnel

(Figs. 3 and 4). The airfoil was mounted by fitting aluminum endplates into a plexiglass and aluminum turntable that was bolted to the insert walls. Angle of attack was varied by loosening the turntable bolts and rotating the airfoil to the desired angle using calibration lines scribed on the turntable.

Two pitot-static probes--one above and one below the airfoil--were attached to the insert wall upstream of the airfoil to determine free-stream dynamic pressure. The static pressure measured by a pitot-static probe in the test section is strongly influenced by the pressure field set up by the airfoil and the leading edge of the parallel wall inserts. Previous results of potential flow studies indicated that these pressure field influences could be minimized by properly placing the pitot-static probes and by taking the test section dynamic pressure to be the average of the dynamic pressures measured by the two probes. This averaging technique has been proven valid in several recent tests over a wide range of angles of attack.

Boundary-layer control was applied to the insert walls near the airfoil to minimize three-dimensional effects by preventing boundary-layer separation of these walls. This was achieved with two wall blowing slots located near the airfoil-wall junction at midchord on the upper surface. The source of wall blowing air was a 90-psi supply system with air mass flow controlled by a Leslie pneumatic control valve and measured by a separate venturi flowmeter. Air reached the wall slots via 1-in.-diameter hoses connected to two 1.5-in.-diameter hoses fed through the tunnel floor. Wall blowing slot gaps were fixed at a nominal opening of 0.03 in. The wall blowing rate was determined by setting a nominal tunnel dynamic pressure (15 psf) and observing the airflow on tufts near the airfoil-wall junctions and across the span on the upper surface. Wall blowing was adjusted until the movement of the tufts indicated the flow was attached. This wall blowing setting was held constant for most tunnel runs. Because of concern that the blowing was excessive

at the lowest Reynolds number conditions (0.25 and 0.4 x 10^6), data were taken with and without blowing at these conditions. Flow visualization studies at these Reynolds numbers indicated that the flow was more two-dimensional without wall blowing; therefore, only the results of the data taken without wall blowing are presented. (The wall blowing increased the airfoil lift slightly and had no measurable effect on the drag.)

A 24-in. long wake rake (Fig. 4c) with 60 total and 10 static pressure tubes (0.042 in. outer diameter) was mounted vertically two chord lengths downstream of the airfoil. The total pressure tubes were arranged such that the tube distribution was most dense (0.25 in. spacing) near the center of the rake.

All of the experimental data were collected on a Tektronix 4052 computer system through a TransEra, Model 752, 16-channel analog-to-digital converter (ADC). The airfoil surface, wake rake, and tunnel dynamic pressures were measured using four 1-psi differential pressure transducers referenced to atmospheric pressure. The transducer voltages were amplified and filtered through Vishay amplifiers, fed into the ADC, and read by the computer. Pressures from the airfoil, wake rake, and pitot-static probes were connected to the transducers using four S-type Scanivalve modules, each capable of scanning 48 individual pressures under computer control. A reference pressure system employing a Mensor pressure standard was used to check variance of the transducers during acquisition of each data point.

The model pressure distribution as well as the wake rake total and static pressure distributions were available for computer screen display and hard copy at run time. The data were stored on floppy disk for a more complete data reduction at a later time. The data reduction, analysis, and report figure generation were also accomplished on the Tektronix 4052 computer.

The wall blowing flow rate was measured with a venturi meter. The upstream

and throat orifices were connected to opposite sides of a 10-psi differential transducer. The upstream orifice was also connected to a 200-psi differential pressure transducer referenced to atmospheric pressure. Two Chromel-Alumel type-K thermocouples were used to measure temperatures. One thermocouple was located in the 90-psi air system just upstream of the wall blowing venturi flowmeter. The second thermocouple, located in the ceiling of the 3- by 8-ft test section, recorded tunnel temperature. Both thermocouples were wired to 125°F reference junctions connected to separate channels on the ADC.

EXPERIMENTAL PROCEDURE

The required data (lift, drag, and moment coefficients) were calculated from pressures measured on the airfoil surface and in the wake. The two test parameters varied were angle of attack and Reynolds number.

The wake drag was determined in a conventional manner from wake rake measurements using the method described by Jones.[2]

$$C_d = 2 \int_{y=-\infty}^{\infty} \sqrt{\frac{P_{o_2} - P_2}{q_\infty}} \left(1 - \sqrt{\frac{P_{o_2} - P_\infty}{q_\infty}}\right) \left\{1 + \frac{M_\infty^2}{8} \left[3 \frac{P_2 - P_\infty}{q_\infty} + 3 - 2\gamma - 2 \frac{P_{o_2} - P_\infty}{q_\infty} - (2\gamma - 1) \sqrt{\frac{P_{o_2} - P_\infty}{q_\infty}}\right]\right\} d\left(\frac{y}{c}\right). \quad (1)$$

where P_{o_∞}, P_{o_2}, and P_2 represent free-stream total, wake total, and wake static pressures. A typical wake total pressure distribution is shown in Fig. 5.

Section lift and moment about the quarter chord were evaluated by integrating the static pressure measured by pressure orifices along the airfoil surface. Both normal and axial force coefficients (C_n and C_a) were determined so that the section

lift coefficient could be calculated from the relationship

$$C_l = C_n \cos(\alpha) - C_a \sin(\alpha). \quad (2)$$

Section moment coefficient about the quarter chord was calculated as:

$$C_{mc/4} = \oint C_p[(x/c) - 0.25)]d(x/c) + \oint C_p(y/c)d(y/c). \quad (3)$$

RESULTS AND DISCUSSION

In a low Reynolds number flow regime, airfoil performance is highly dependent on low Reynolds number boundary-layer behavior. Key aspects of this behavior include airfoil pressure distribution, transition location, and Reynolds number.

PRESSURE DISTRIBUTIONS

The effect of angle of attack on chordwise pressure distribution for a Reynolds number of 1×10^6 is shown in Fig. 6. A range of angles of attack existed yielding drag values that held nearly constant about the minimum drag value. This "low drag" range of angles was the result of the pressure distributions and their effect on boundary-layer behavior.

The lower limit of the low drag angle-of-attack range occurred between -3 deg and -6 deg where a pressure peak formed on the lower surface near the leading edge; see Fig. 6a. The development of this peak signaled the rapid advancement of transition towards the leading edge. At an angle of attack of 0 deg ($C_\ell = 0.60$), favorable pressure gradients existed on both surfaces to about $x/c = 0.6$; see Fig. 6b. The upper limit of the low drag range was between 6 deg and 9 deg where a pressure peak occurred on the upper surface near the leading edge (Figs. 6b and 6c). The pressure peak increased with increasing angle of attack. Consequently, the transition point moved forward and, ultimately, led to turbulent trailing edge

separation at 9 deg.

The three pressure distributions in Fig. 6c show regions of constant pressure near the trailing edge on the upper surface that are characteristic of boundary-layer separation. The absence of a constant pressure region at lower angles of attack is verification that stall has taken place at the angles greater than 6 deg. (This trailing edge separation was also verified with flow visualization.) It can be assumed that there will be a substantial increase in drag from 6 deg to 9 deg. As the angle of attack increases from 9 deg to 15 deg, the trailing edge separation moves forward.

TRANSITION LOCATION

The method for determining the transition location for most angles tested involved locating the sudden pressure increase in the chordwise pressure distribution (Fig. 7a). In these regions a laminar separation bubble has formed, and the pressure increase indicates the transition of the free shear layer before turbulent reattachment. The laminar separation bubble is caused by a slightly adverse pressure gradient downstream of the minimum pressure on the surface.

It is interesting to note that Wortmann was one of the first airfoil designers to incorporate a transition ramp--a short run of slight adverse pressure gradient ahead of the pressure recovery region--to induce transition before undergoing the steep pressure recovery gradient. Transition ramps that can operate successfully over a wide range of Reynolds numbers and angles of attack are difficult to design. It is likely that the Wortmann airfoil was designed to operate at higher Reynolds numbers where, perhaps, these midchord laminar separation bubbles might have been avoided.

The existence of a laminar separation bubble was verified by flow visuali-

zation using the techniques of mixing oil with flourescent dye and of suspending magnesium carbonate (a white powder) in paint thinner. At 9 deg, where there is no bubble on the upper surface, an oil flow technique was used to chart transition; see Fig. 7b. Varied drying rates of the white powder solution corresponding to laminar and turbulent boundary layers were used to verify the oil flow results.

The variation of section lift coefficient with transition location is shown in Fig. 8. The transition point progresses forward with increasing lift coefficient on the upper surface and toward the trailing edge on the lower surface.

REYNOLDS NUMBER EFFECTS

Figure 9 shows the variation of lift coefficient with transition location at two Reynolds numbers. At 3 deg (C_ℓ = 0.95), the location of transition moves forward approximately x/c = 0.06 on both upper and lower surfaces. The slopes of the variation of transition with lift are comparable for both Reynolds numbers.

The effect of Reynolds number on airfoil section characteristics is shown in Figs. 10a through 10c. The angle of attack for zero lift is approximately -5 deg. The lift and moment coefficients are relatively insensitive to Reynolds number variation.

The variation of section drag with Reynolds number and angle of attack is shown in Fig. 11. Figures 10 and 11 show a trend of decreasing drag coefficient with increasing Reynolds number for angles where there is no trailing edge separation. The approximate boundaries of the low drag range are -6 deg and 6 deg. The rapid advancement of transition toward the leading edge is at 6 deg. The advancement of transition is displayed by the drag coefficient values increasing rapidly at 6 deg and Reynolds numbers above 0.8×10^6. This drag increase corresponds to a turbulent boundary layer over an increasing amount of the upper surface. The drag

begins a sharp increase at -6 deg and Reynolds number above 0.4×10^6, indicating transition has advanced toward the leading edge of the lower surface. At 9, 12, and 15 deg, the trailing edge separation moves forward with increases in Reynolds number.

COMPARISON WITH OTHER DATA

The variation of section lift coefficient with transition location at a Reynolds number of approximately 1×10^6 compares closely with the data of Althaus[1] (Fig. 12). The angle of attack for zero lift (Reference 1) was about 0.6 deg greater than the data shown for this experiment (Fig. 13a). The shift of the zero lift angle suggests that the method of altering the design coordinates in the present model (see MODEL DESCRIPTION) may have succeeded in preserving more camber than on the model tested by Althaus.[1] The increase in the nose-down pitching moment also suggests an increased amount of camber on the present model (Fig. 13b). The drag curves compare closely at a Reynolds number of approximately 1×10^6 (Fig. 13c).

COMPARISON WITH THEORETICAL DATA

The Transition Analysis Program System (TAPS)[3,4] was run using the design coordinates of Althaus.[1] The chordwise pressure distributions are compared with the resulting potential flow solution at $C_\ell = 0.96$ in Fig. 14. The lift curve produced using TAPS is shown for several angles of attack in Fig. 15. As expected, the theoretical airfoil results are shifted further to the left. The lift curve slope is similar to the present data, and the angle of zero lift of the potential flow solution is -5.63 deg.

A boundary-layer analysis was conducted with TAPS using the potential flow pressure distribution for a specified angle of attack. The Squire-Young method was employed to calculate a theoretical drag coefficient. Following the suggestion of Cebeci,[5] flow properties used in the formula were evaluated at $x/c = 0.095$. Figure

16 shows the theoretical drag polar compared with the test data.

Wortmann[6] states that drag values can be approximated by multiplying flat-plate drag values by 1+2t/c. A drag curve obtained with this method is included in Fig. 11. The agreement is quite good for the non-stall angles of attack. Flat-plate boundary-layer transition is assumed to occur at x/c = 0.55, and the virtual origin of the turbulent boundary layer is located such that the momentum thickness is continuous at the transition point.

SUMMARY

An investigation was performed in the DTNSRDC south subsonic wind tunnel to determine the low-speed, two-dimensional aerodynamic characteristics of the Wortmann FX61-184 airfoil. The experiment was conducted with a chord Reynolds number ranging from approximately 0.25 to 1.0 x 10^6. These data results have been compared with the test data of Althaus.[1]

1. At a Reynolds number of 1 x 10^6, the drag data compares closely with that of Althaus.[1]

2. The lift and moment data indicate that the model tested in this experiment has slightly more camber than the model tested by Althaus.[1]

3. Transition on both upper and lower surfaces is in the form of laminar separation bubbles at the low drag angles of attack and Reynolds numbers between 0.25 and 1.0 x 10^6.

4. The occurrence of transition by the bubble mechanism on both surfaces of the airfoil in the moderate angle-of-attack range indicates that the airfoil may not have been designed to operate in the Reynolds number range tested in this experiment (below 1.0 x 10^6).

5. The drag change with Reynolds number in the low drag angle-of-attack range is as expected for an airfoil with transition occurring near midchord.

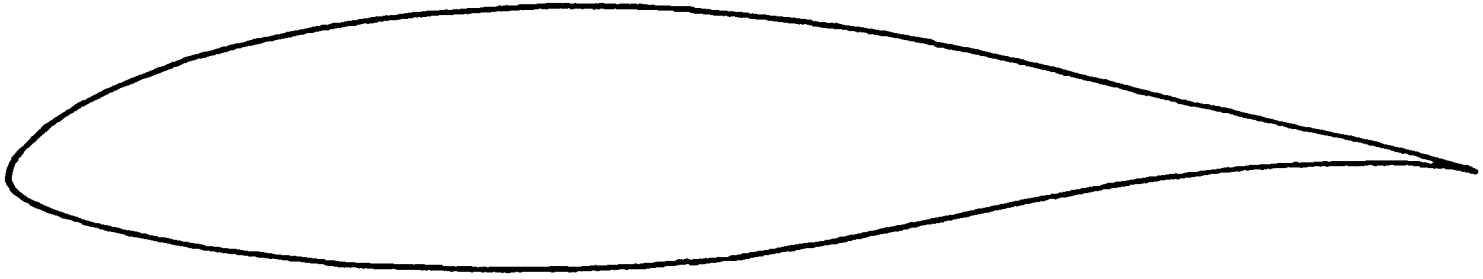

Fig. 1. Wortmann FX61-184 airfoil.

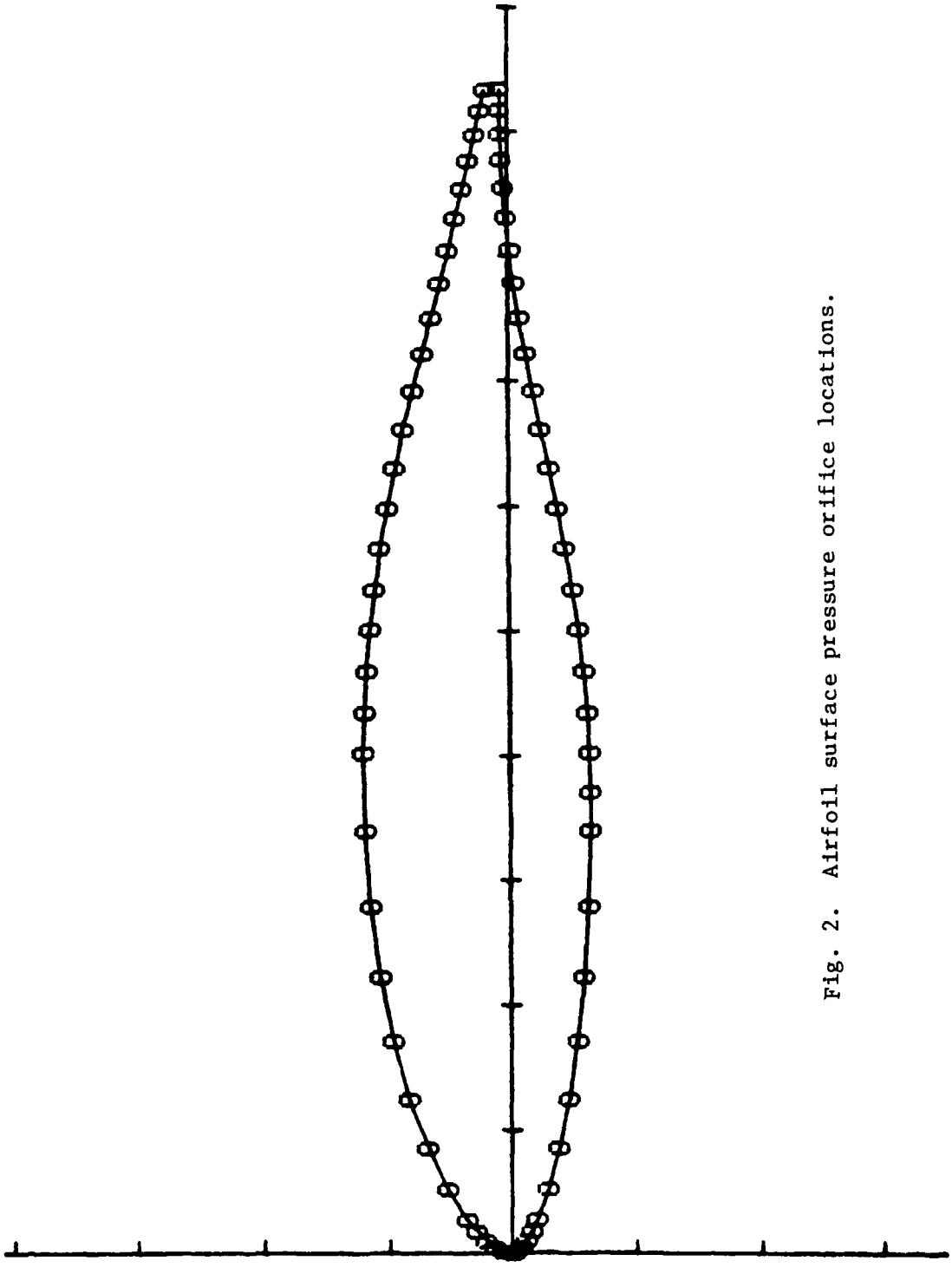

Fig. 2. Airfoil surface pressure orifice locations.

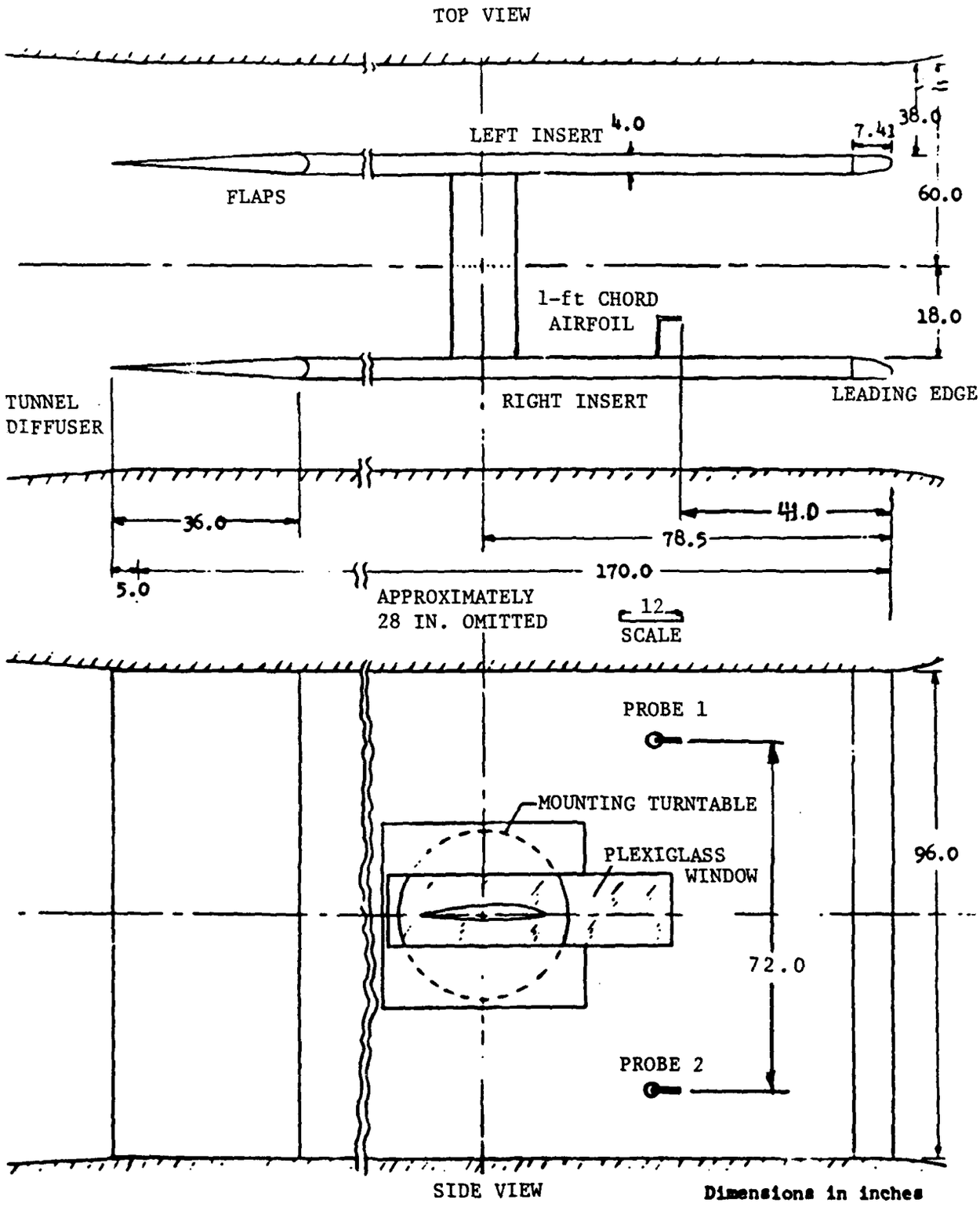

Fig. 3. Subsonic two-dimensional test facility.

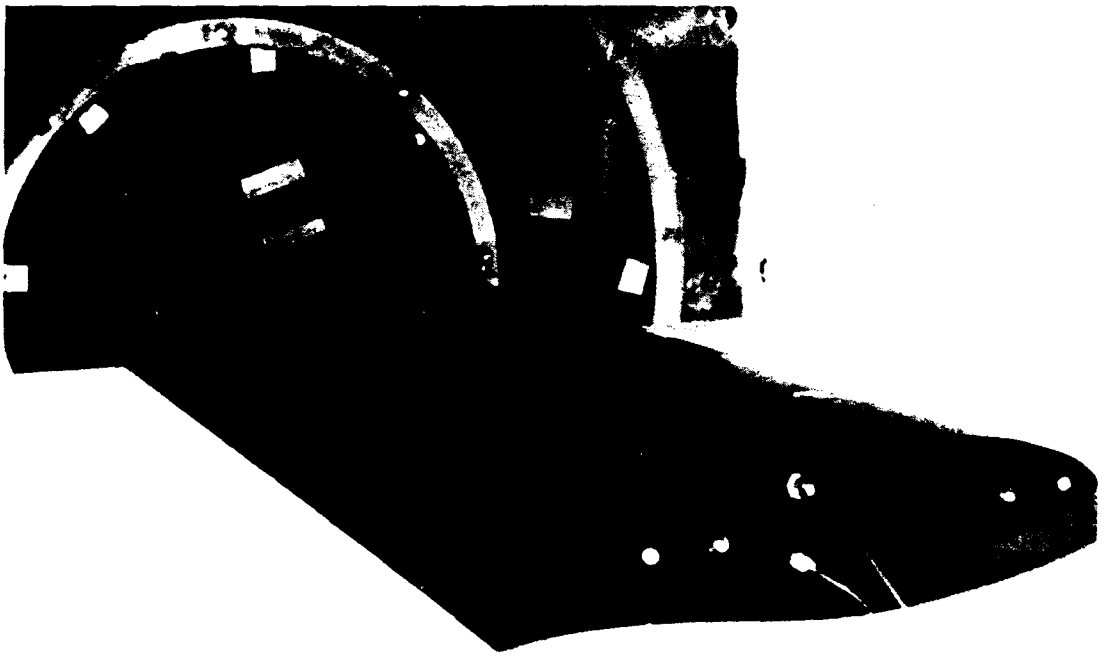

Fig. 4a. Airfoil section.

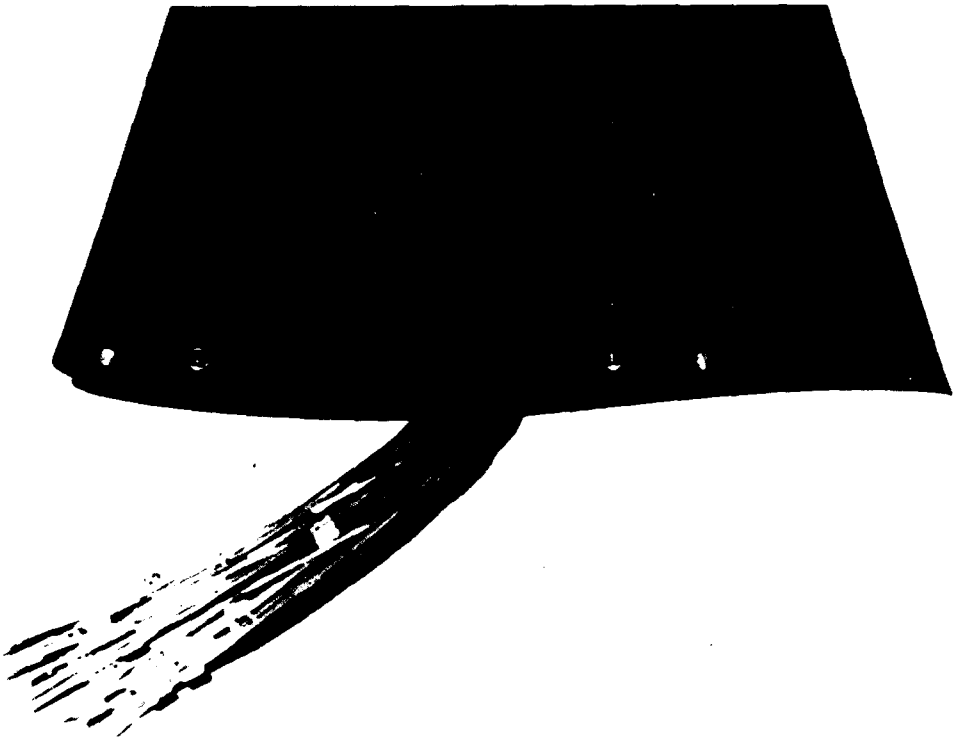

Fig. 4b. Pressure tubing.

Fig. 4. Airfoil and wake rake installation.

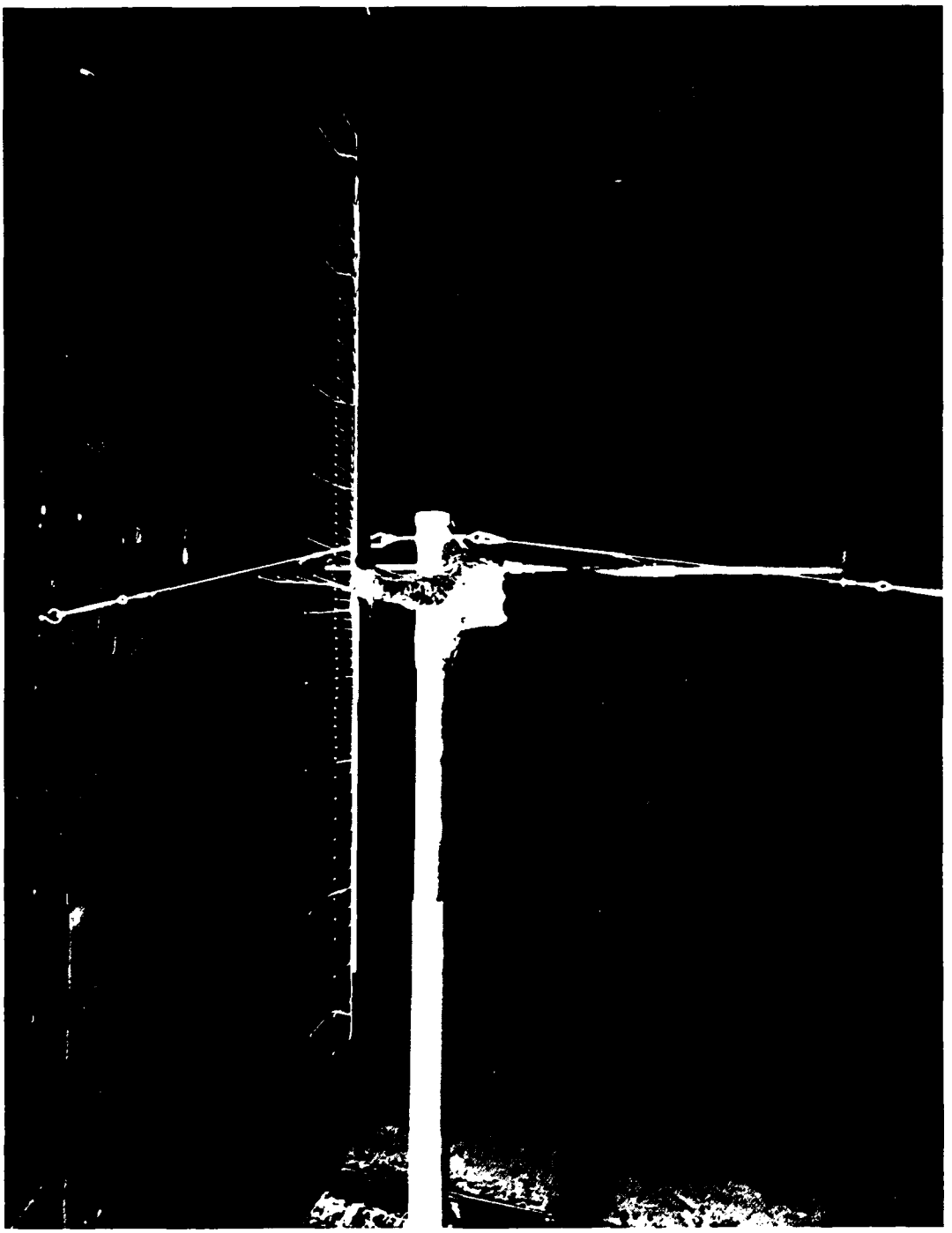

Fig. 4c. Wake rake.

Fig. 4. (Continued)

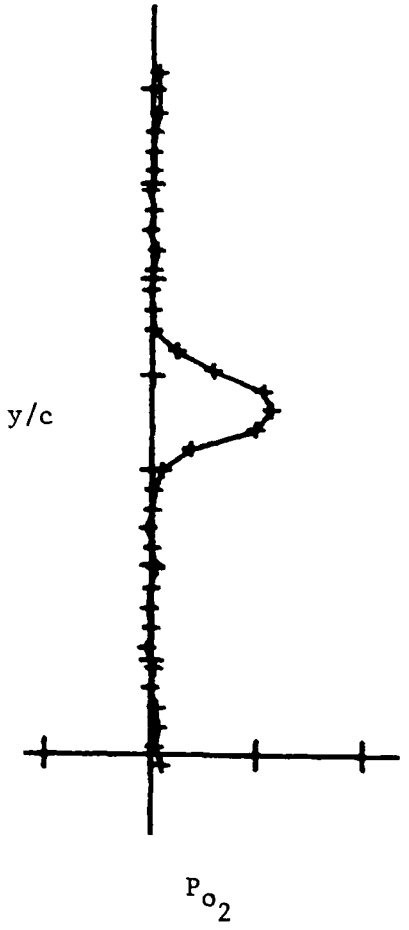

Fig. 5. Typical wake total pressure distribution.

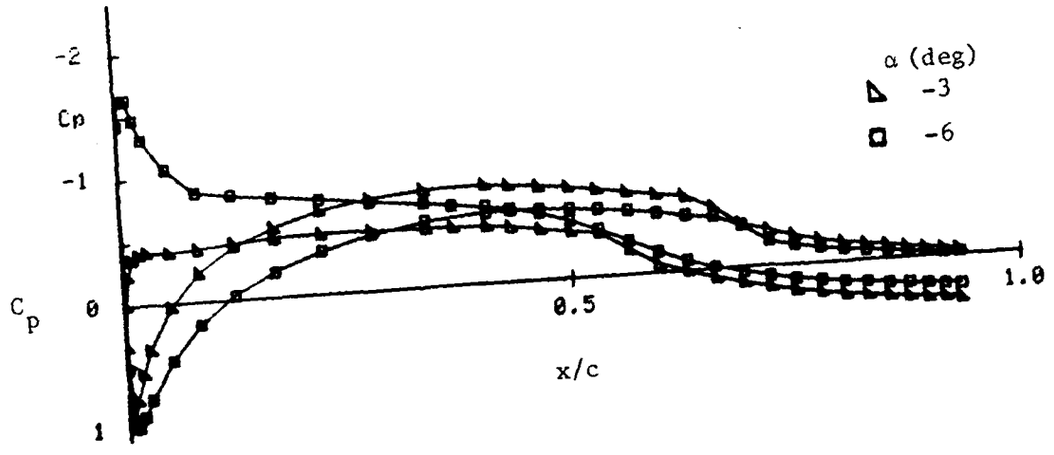

Fig. 6a.

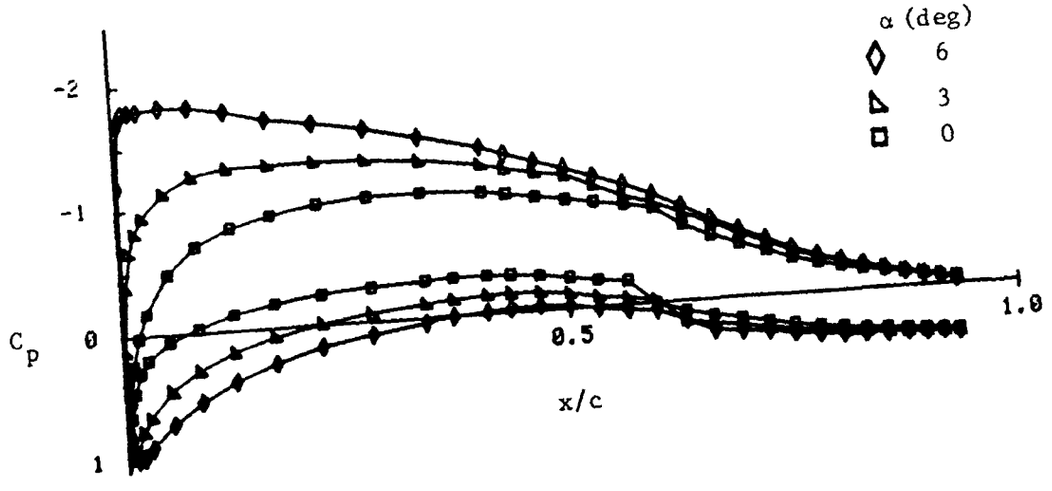

Fig. 6b.

Fig. 6. Effect of angle of attack on chordwise pressure distribution for Re = 1 x 10^6.

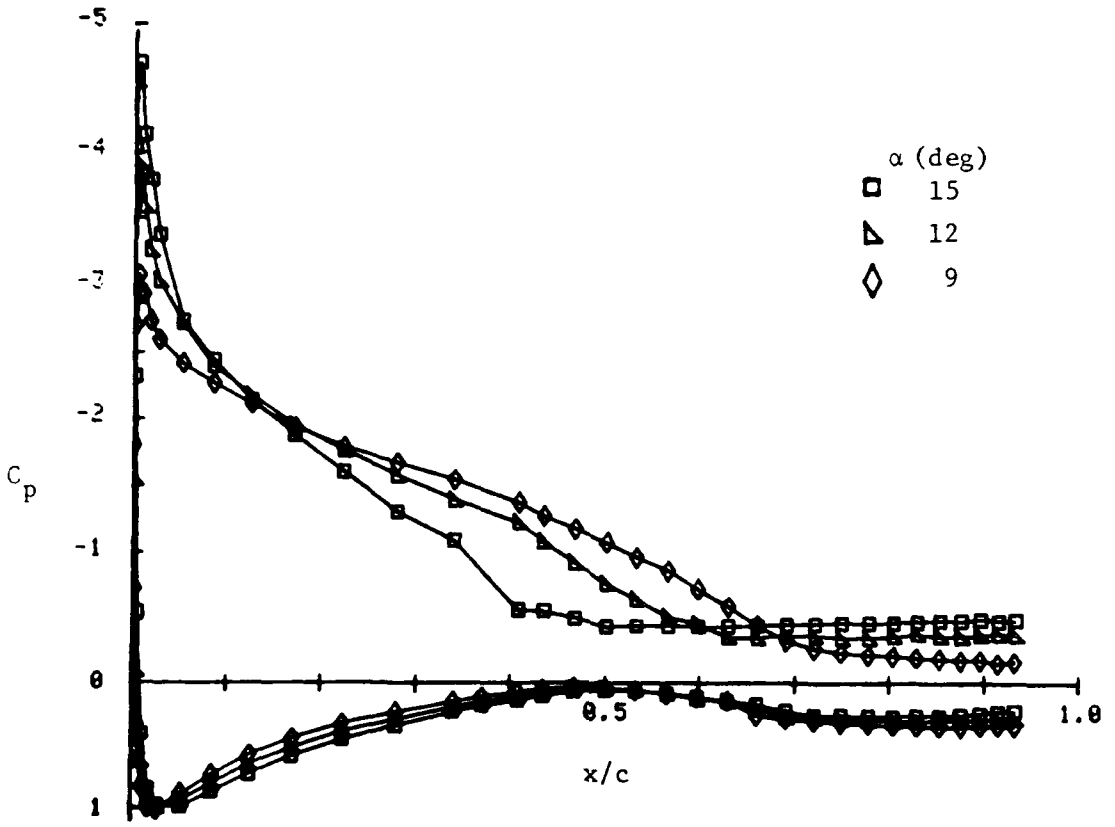

Fig. 6c.

Fig. 6. (Continued)

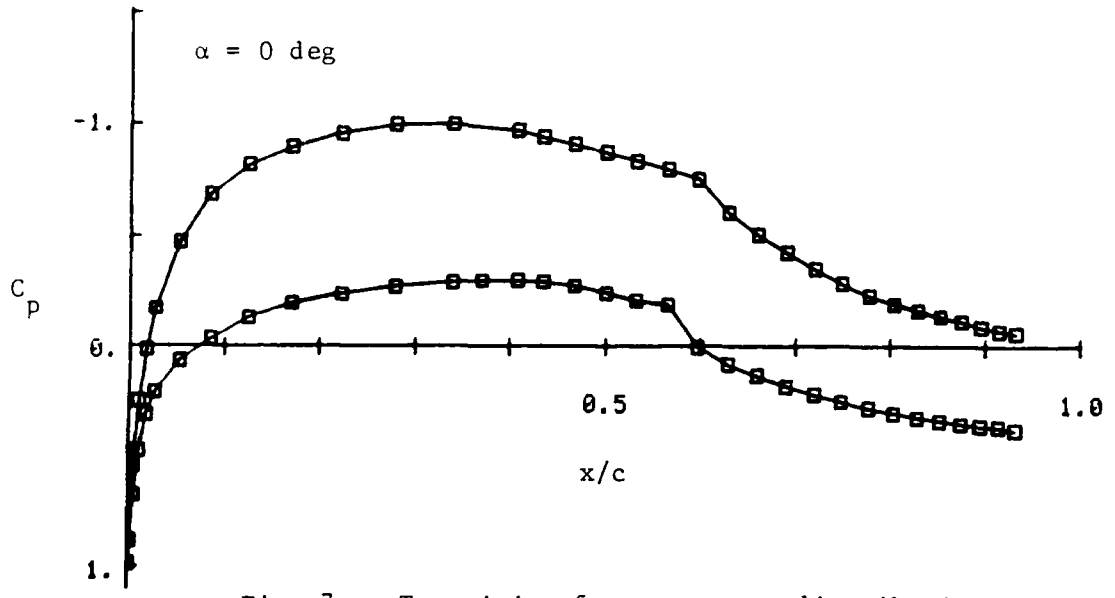

Fig. 7a. Transition from pressure distribution.

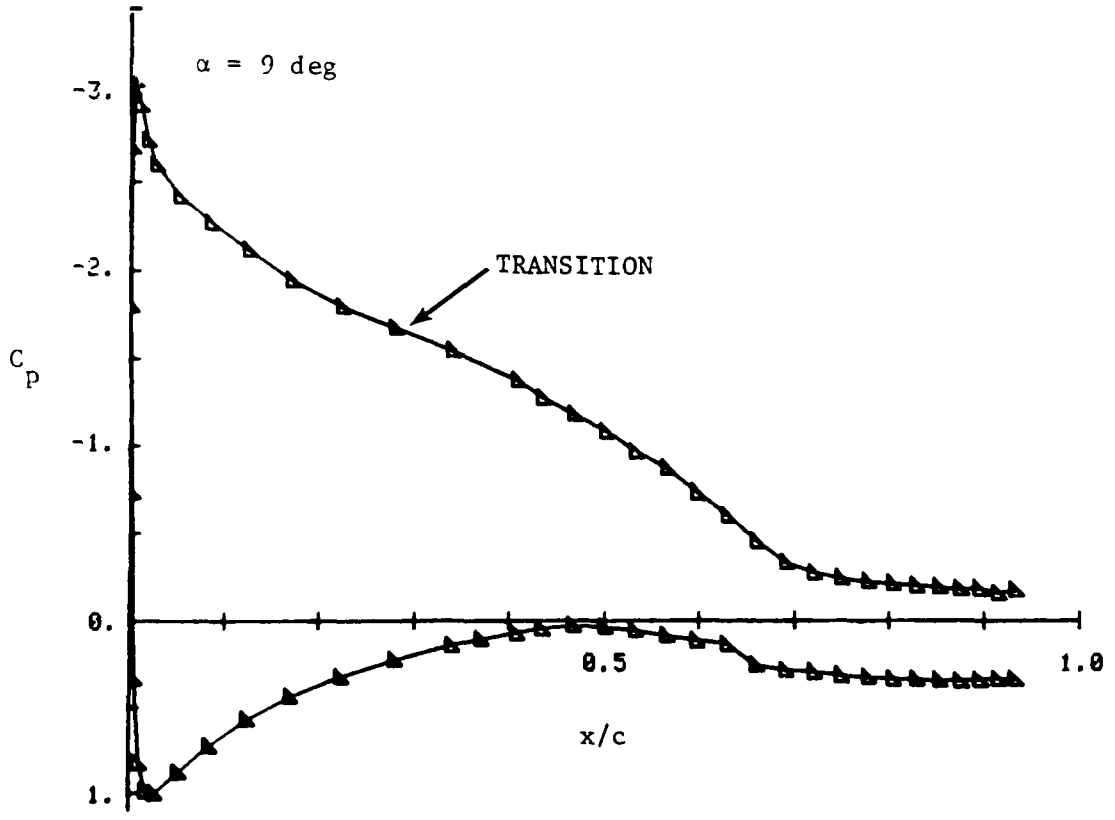

Fig. 7b. Transition from oil flow.

Fig. 7. Effect of chordwise pressure distribution on transition location for Re = 1 x 10^6.

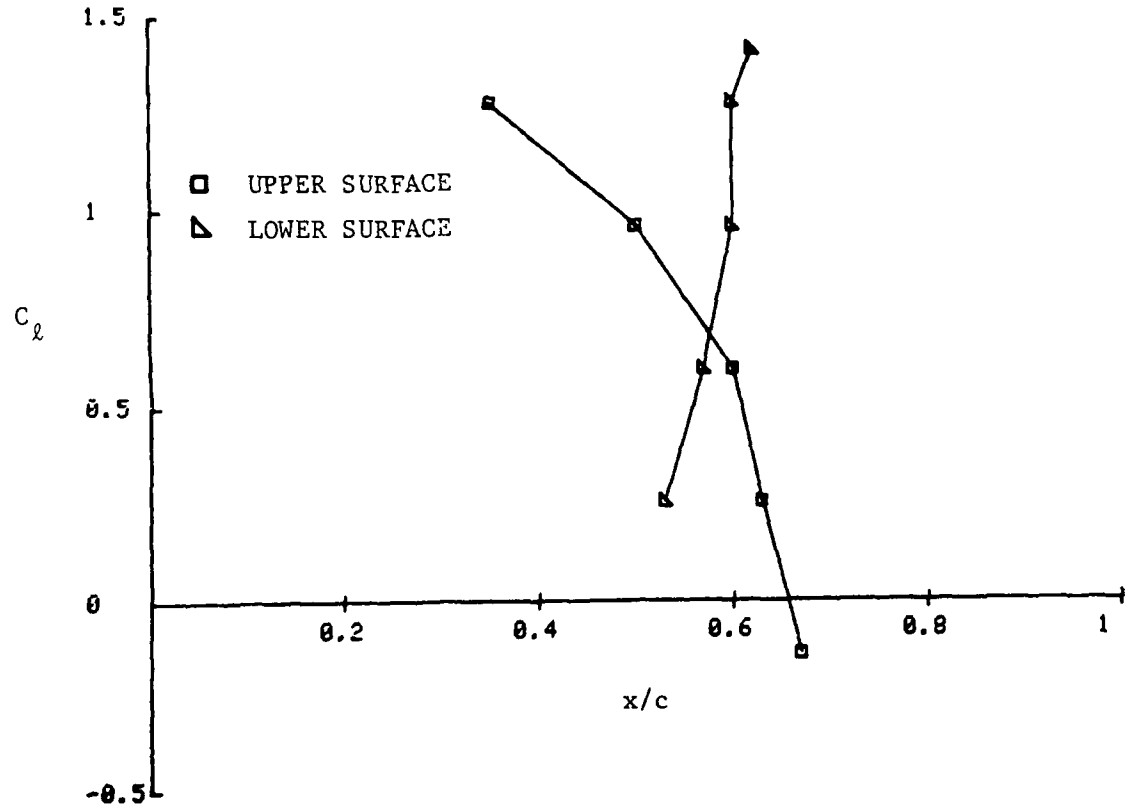

Fig. 8. Variation of section lift coefficient with transition location.

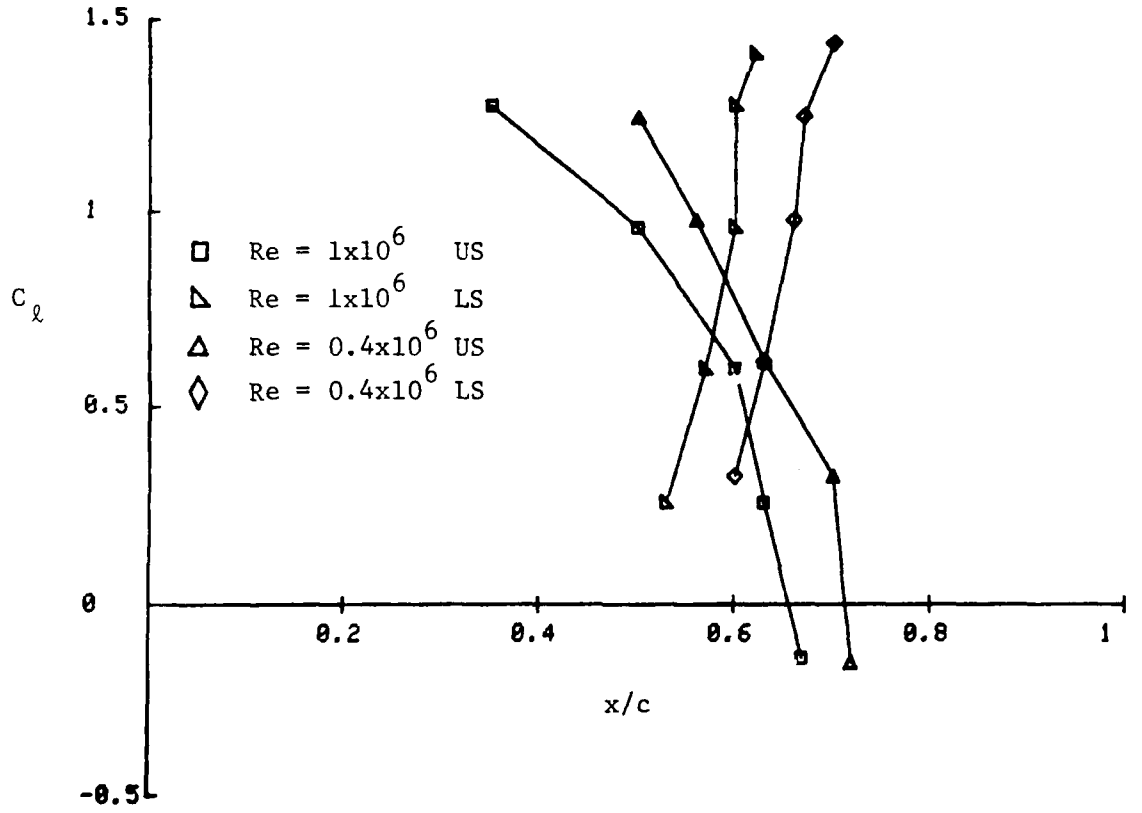

Fig. 9. Effect of Reynolds number on transition location.

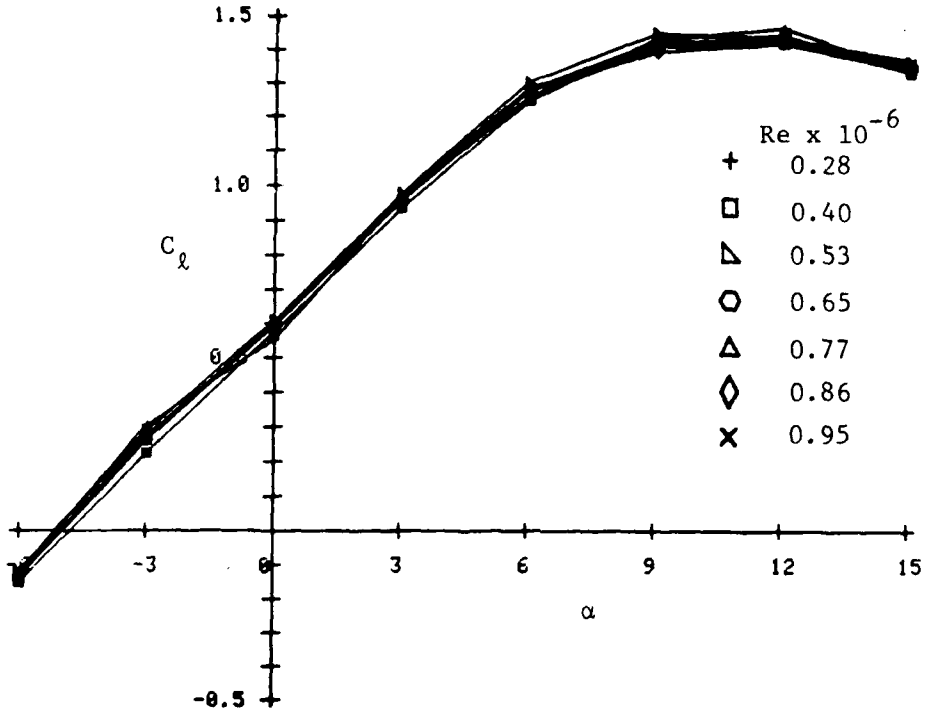

Fig. 10a. Lift coefficient versus angle of attack.

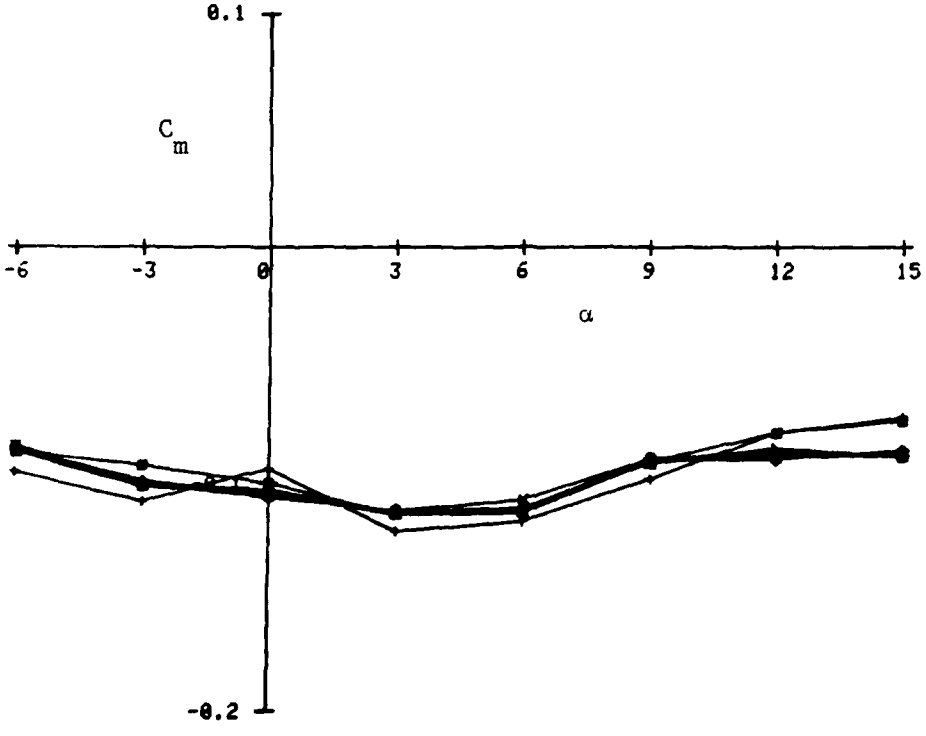

Fig. 10b. Quarter-chord pitching moment coefficient versus angle of attack.

Fig. 10. Effect of Reynolds number on section characteristics.

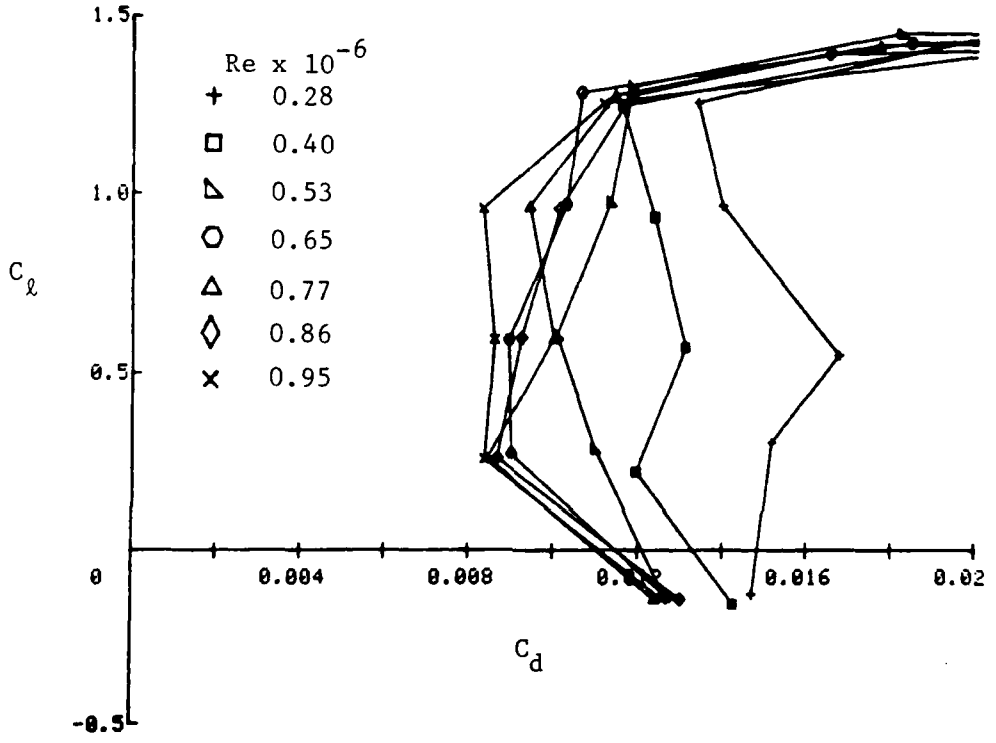

Fig. 10c. Lift coefficient versus drag coefficient.

Fig. 10. (Continued)

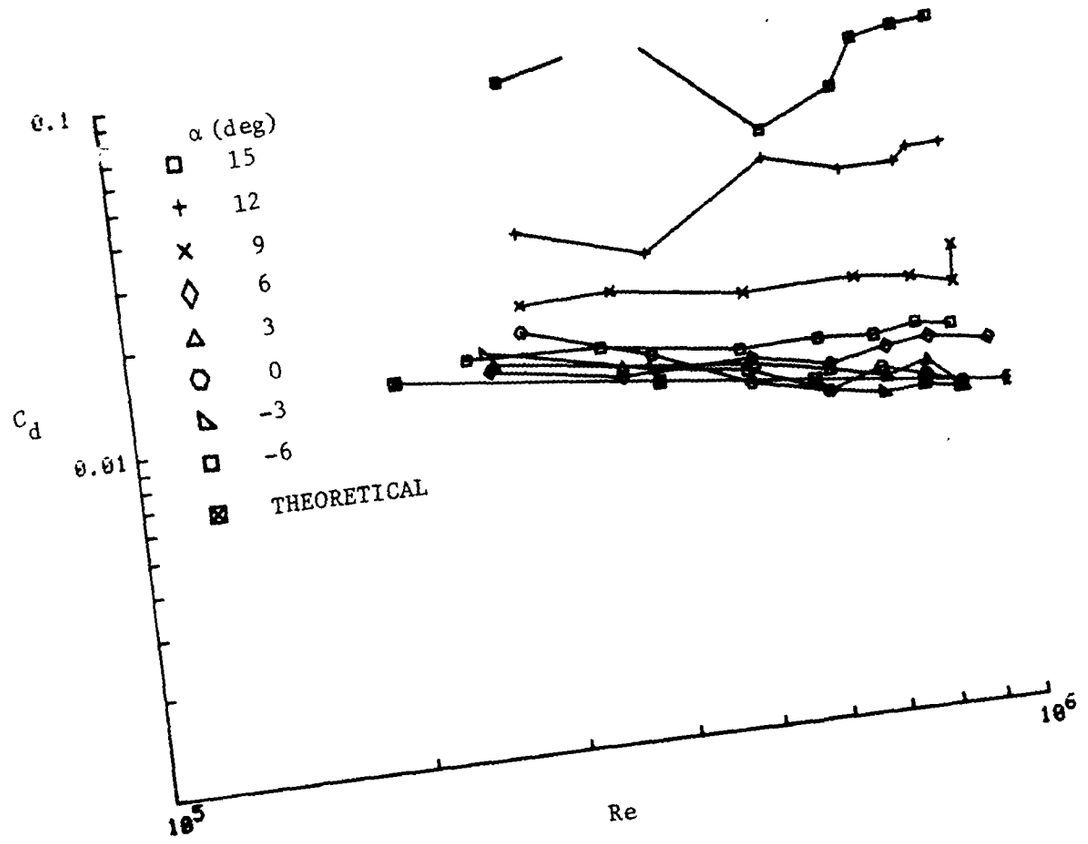

Fig. 11. Variation of section drag with Reynolds number.

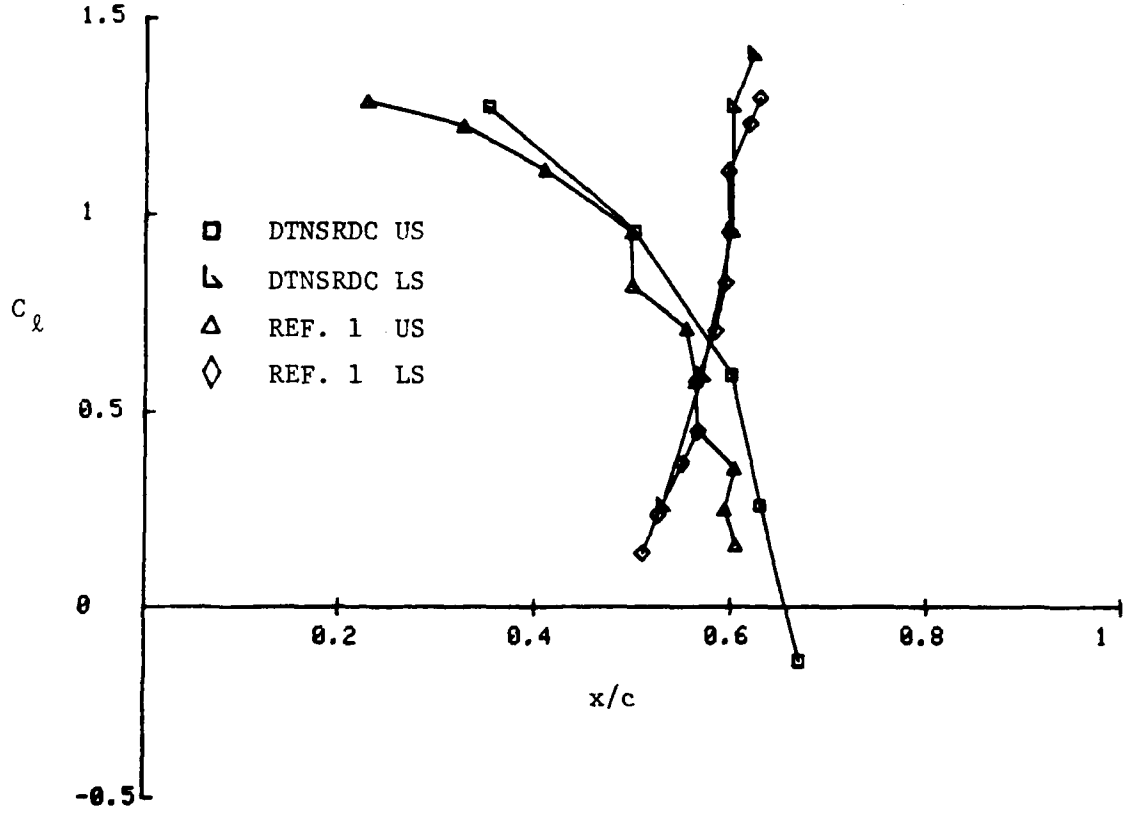

Fig. 12. Comparison of transition location for Re = 1 x 10^6.

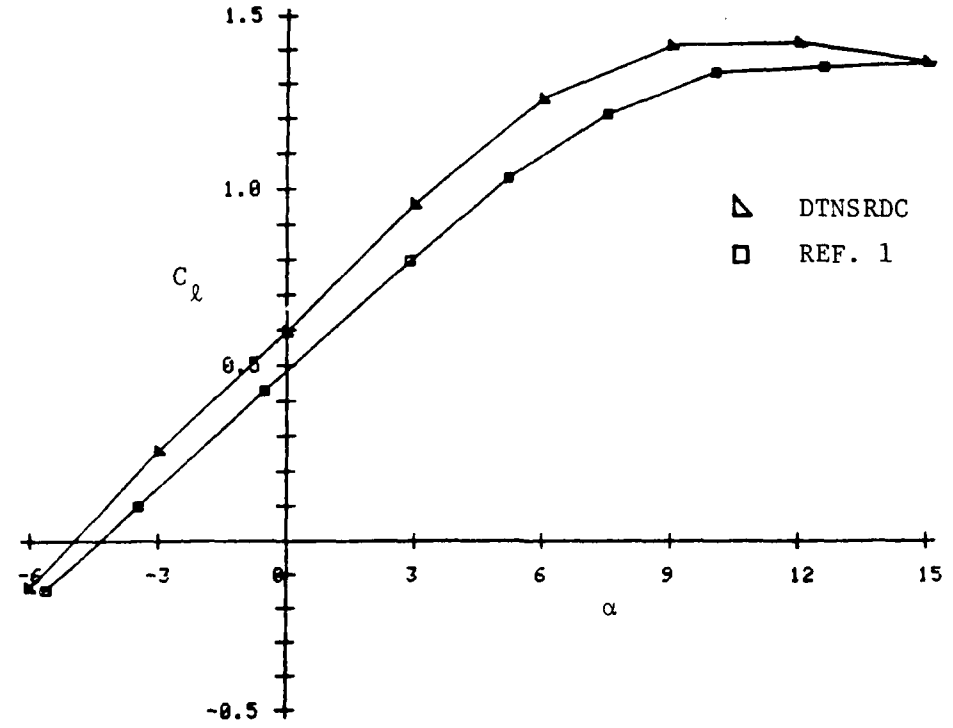

Fig. 13a. Lift coefficient versus angle of attack.

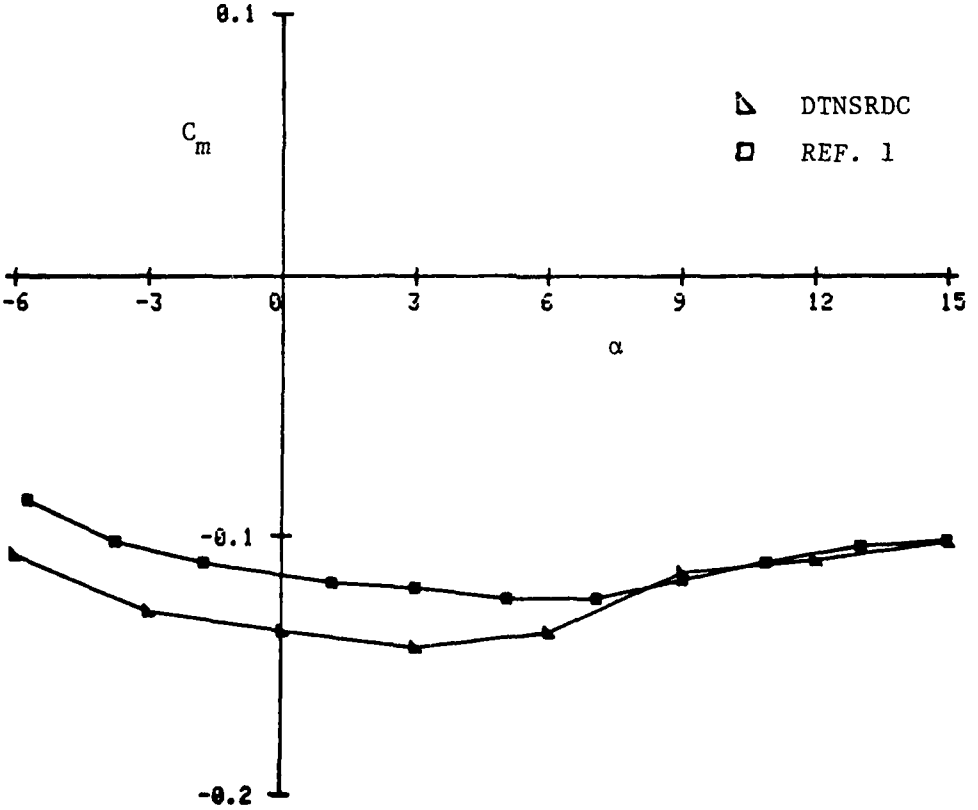

Fig. 13b. Quarter-chord pitching moment coefficient versus angle of attack.

Fig. 13. Comparison of section characteristics for Re = 1 x 10^6.

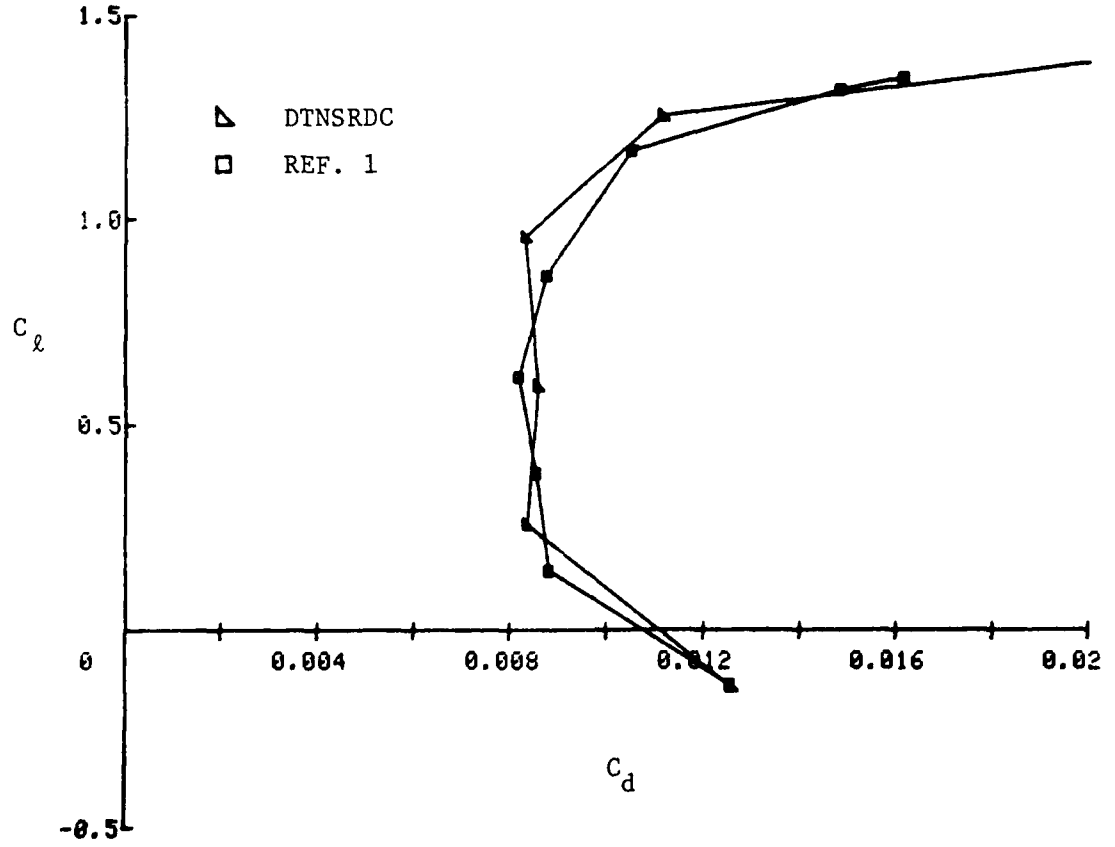

Fig. 13c. Lift coefficient versus drag coefficient.

Fig. 13. (Continued)

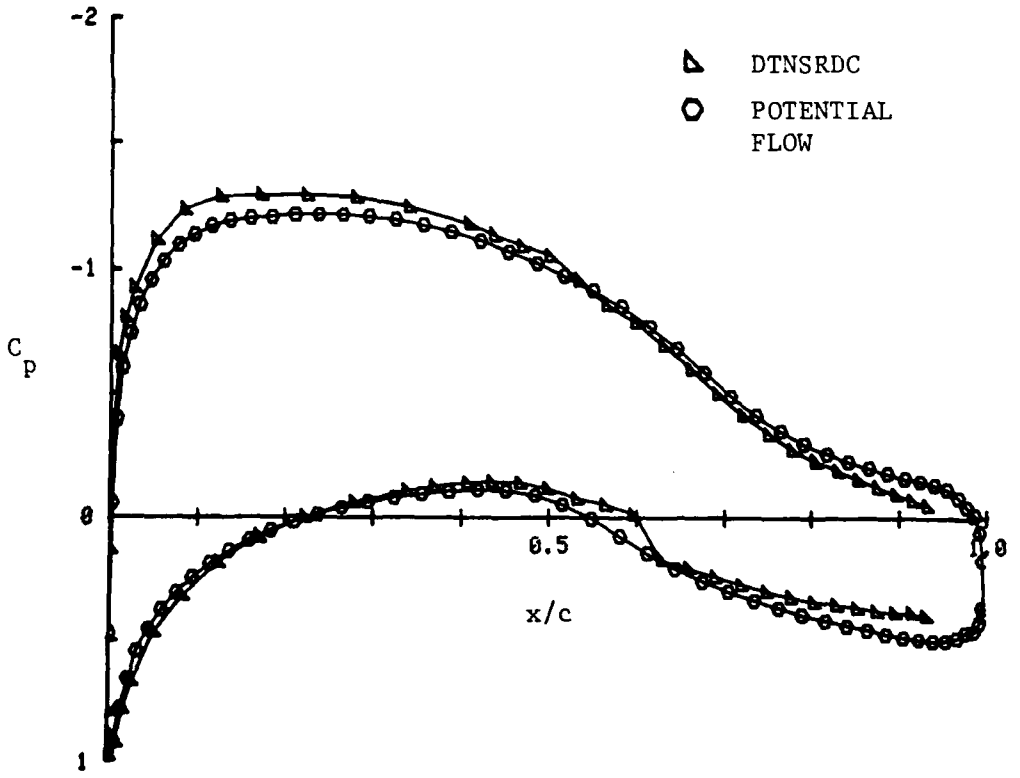

Fig. 14. Comparison of chordwise pressure distribution with potential flow solution at C_ℓ = 0.96.

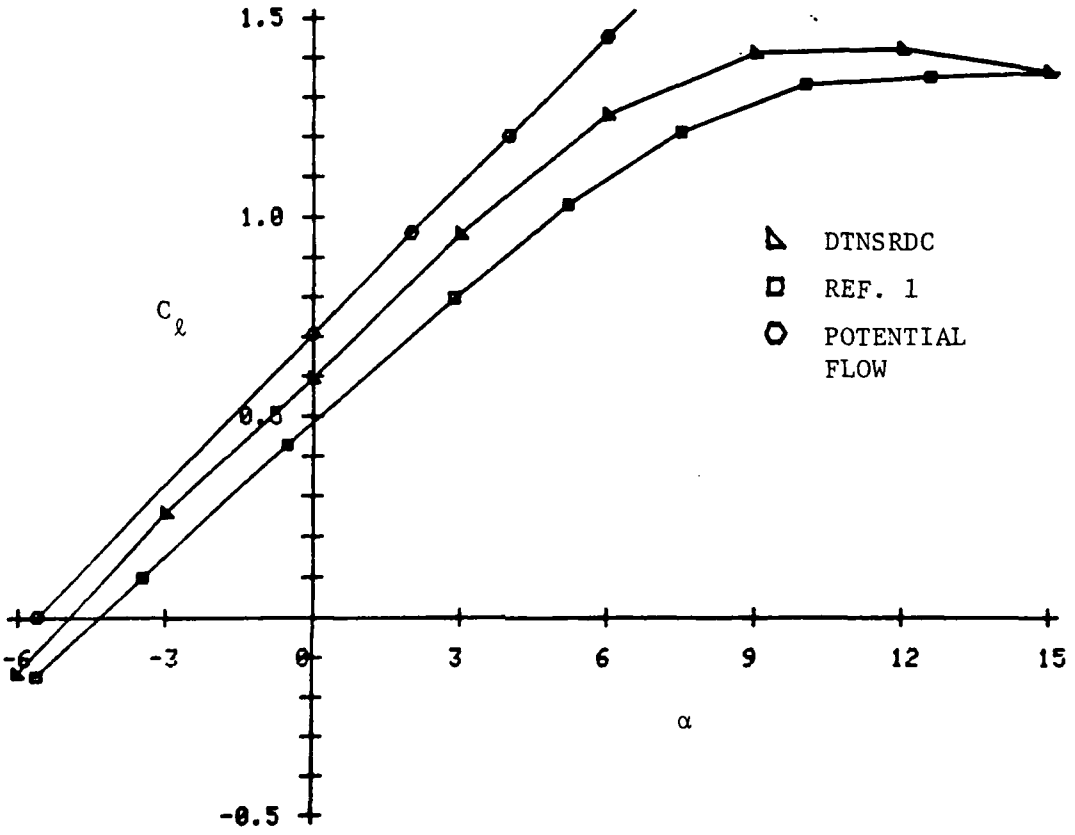

Fig. 15. Comparison of potential flow lift curve with test data.

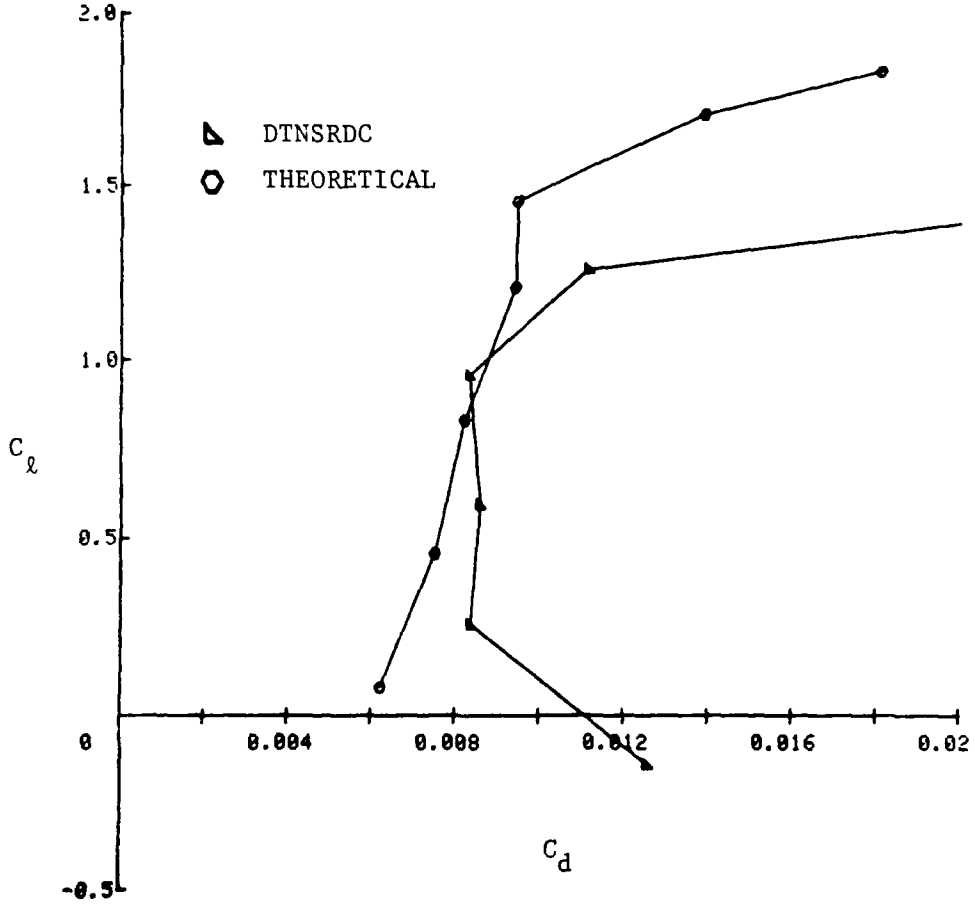

Fig. 16. Comparison of theoretical section drag with test data.

Table 1. Design airfoil section coordinates.

x/c	z_u/c	z_l/c	x/c	z_u/c	z_l/c
0.00000	0.00000	0.00000	0.53274	0.10974	-0.05042
0.00102	0.00812	-0.00243	0.56525	0.10511	-0.04462
0.00422	0.01520	-0.00671	0.59750	0.09958	-0.03817
0.00960	0.02251	-0.01103	0.62938	0.09323	-0.03148
0.01702	0.03006	-0.01538	-0.66074	0.08619	-0.02495
0.02650	0.03790	-0.01975	0.69133	0.07877	-0.01888
0.03802	0.04598	-0.02414	0.72115	0.07125	-0.01340
0.05158	0.05407	-0.02851	0.74995	0.06395	-0.00853
0.06694	0.06205	-0.03285	0.77773	0.05695	-0.00431
0.08422	0.06980	-0.03713	0.80435	0.05035	-0.00075
0.10330	0.07724	-0.04129	0.82970	0.04417	0.00215
0.12403	0.08427	-0.04529	0.85350	0.03842	0.00440
0.14643	0.09082	-0.04906	0.87590	0.03309	0.00601
0.17037	0.09681	-0.05251	0.89644	0.02819	0.00702
0.19558	0.10228	-0.05560	0.91571	0.02369	0.00747
0.22221	0.10710	-0.05831	0.93299	0.01957	0.00742
0.24998	0.11127	-0.06055	0.94848	0.01580	0.00696
0.27891	0.11466	-0.06230	0.96192	0.01234	0.00610
0.30861	0.11724	-0.06349	0.97344	0.00920	0.00494
0.33933	0.11893	-0.06407	0.98291	0.00640	0.00361
0.37056	0.11973	-0.06400	0.99034	0.00408	0.00244
0.40243	0.11958	-0.06320	0.99571	0.00218	0.00129
0.43469	0.11850	-0.06156	0.99891	0.00079	0.00031
0.46733	0.11646	-0.05895	1.00000	0.00000	0.00000
0.49997	0.11355	-0.05524			

Table 2. Model section coordinates.

x/c	z_u/c	z_l/c	x/c	z_u/c	z_l/c
0.0000	0.0000	0.0000	0.5327	0.1104	-0.0511
0.0010	0.0081	-0.0024	0.5653	0.1058	-0.0453
0.0042	0.0152	-0.0067	0.5975	0.1003	-0.0389
0.0096	0.0225	-0.0110	0.6294	0.0940	-0.0323
0.0170	0.0301	-0.0154	0.6607	0.0870	-0.0258
0.0265	0.0379	-0.0198	0.6913	0.0796	-0.0197
0.0380	0.0460	-0.0242	0.7212	0.0722	-0.0143
0.0516	0.0541	-0.0286	0.7500	0.0649	-0.0095
0.0669	0.0621	-0.0329	0.7777	0.0579	-0.0053
0.0842	0.0699	-0.0372	0.8044	0.0514	-0.0018
0.1033	0.0774	-0.0414	0.8297	0.0452	0.0011
0.1240	0.0844	-0.0454	0.8535	0.0395	0.0033
0.1464	0.0910	-0.0492	0.8759	0.0342	0.0049
0.1704	0.0970	-0.0527	0.8964	0.0293	0.0059
0.1956	0.1025	-0.0558	0.9157	0.0248	0.0063
0.2222	0.1074	-0.0586	0.9332	0.0207	0.0063
0.2500	0.1116	-0.0609	0.9485	0.0170	0.0058
0.2789	0.1150	-0.0627	0.9619	0.0135	0.0049
0.3086	0.1176	-0.0639	0.9734	0.0104	0.0037
0.3393	0.1194	-0.0645	0.9829	0.0076	0.0024
0.3706	0.1202	-0.0645	0.9903	0.0053	0.0012
0.4024	0.1201	-0.0637	0.9957	0.0034	0.0000
0.4347	0.1190	-0.0621	0.9989	0.0020	-0.0009
0.4673	0.1170	-0.0595	1.0000	0.0013	-0.0013
0.5000	0.1142	-0.0559			

REFERENCES

1. Althaus, D., Stuttgarter ProfilKatalog I, Stuttgart University, Germany (1972).
2. Schlicting, H., "Boundary Layer Theory," Sixth Edition, McGraw-Hill Book Company, New York (1968), pp. 711-714.
3. Gentry, A.E., "The Transition Analysis Program System: Volume 1 - User's Manual," McDonnell-Douglas Corporation Report MDC J7255/01 (Jun 1976).
4. Gentry, A.E. and A.R. Wazzan, "The Transition Analysis Program System: Volume 2 - Program Formulation and Listings," McDonnell-Douglas Corporation Report MDC J7255/02 (Jun 1976).
5. Cebeci, T. and A.M.O. Smith, "Calculation of Profile Drag of Airfoils at Low Mach Numbers," Journal of Aircraft, Vol. 5, No. 6 (Nov-Dec 1968).
6. Wortmann, F.X., "A Critical Review of the Physical Aspects of Airfoil Design at Low Mach Numbers," in: Motorless Flight Research-1972, J.L. Nash, Ed., NASA CR 2315 (Nov 1973).